J Neurophysiol 103: 543–556, 2010.
First published November 18, 2009; doi:10.1152/jn.00656.2009.

Saccadic Compensation for Smooth Eye and Head Movements During Head-Unrestrained Two-Dimensional Tracking

P. M. Daye,[1,2] G. Blohm,[3] and P. Lefèvre[1,2]

[1]*Center for Systems Engineering and Applied Mechanics, Université catholique de Louvain, Louvain-la-Neuve;* [2]*Laboratory of Neurophysiology, Université catholique de Louvain, Brussels, Belgium; and* [3]*Centre for Neurosciences Studies, Queen's University, Kingston, Ontario, Canada*

Submitted 27 July 2009; accepted in final form 14 November 2009

Daye PM, Blohm G, Lefèvre P. Saccadic compensation for smooth eye and head movements during head-unrestrained two-dimensional tracking. *J Neurophysiol* 103: 543–556, 2010. First published November 18, 2009; doi:10.1152/jn.00656.2009. Spatial updating is the ability to keep track of the position of world-fixed objects while we move. In the case of vision, this phenomenon is called spatial constancy and has been studied in head-restraint conditions. During head-restrained smooth pursuit, it has been shown that the saccadic system has access to extraretinal information from the pursuit system to update the objects' position in the surrounding environment. However, during head-unrestrained smooth pursuit, the saccadic system needs to keep track of three different motor commands: the ocular smooth pursuit command, the vestibuloocular reflex (VOR), and the head movement command. The question then arises whether saccades compensate for these movements. To address this question, we briefly presented a target during sinusoidal head-unrestrained smooth pursuit in darkness. Subjects were instructed to look at the flash as soon as they saw it. We observed that subjects were able to orient their gaze to the memorized (and spatially updated) position of the flashed target generally using one to three successive saccades. Similar to the behavior in the head-restrained condition, we found that the longer the gaze saccade latency, the better the compensation for intervening smooth gaze displacements; after about 400 ms, 62% of the smooth gaze displacement had been compensated for. This compensation depended on two independent parameters: the latency of the saccade and the eye contribution to the gaze displacement during this latency period. Separating gaze into eye and head contributions, we show that the larger the eye contribution to the gaze displacement, the better the overall compensation. Finally, we found that the compensation was a function of the head oscillation frequency and we suggest that this relationship is linked to the modulation of VOR gain. We conclude that the general mechanisms of compensation for smooth gaze displacements are similar to those observed in the head-restrained condition.

INTRODUCTION

To experience a stable world in spite of self-motion, we have to take the movements of our eyes and head into account. This is known as *spatial constancy* and has been extensively investigated during saccadic eye movements (Hallett and Lightstone 1976a,b), for head-restrained smooth pursuit (Schlag and Schlag-Rey 2002) and during whole-body rotations (Blouin et al. 1995, 1998; Klier et al. 2005, 2006) and translations (Berthoz et al. 1995; Israel et al. 1997; Klier and Angelaki 2008). Most of these previous studies have considered how spatial constancy is achieved across movements generated by a single motor system. More recently, the mechanisms involved in maintaining a spatially stable internal representation of the world have been examined during combined saccadic and pursuit eye movements (Blohm et al. 2003, 2005a,b, 2006). However, the latter studies were performed with the head restrained (except for Herter and Guitton 1998). In the present study, we sought to consider the saccadic compensation for smooth eye movements in a more natural behavioral condition where the head was free to move.

When the head is restrained, it has been shown that saccades can compensate for smooth pursuit eye movements if the saccadic system is given sufficient time (Blohm et al. 2003, 2005a,b). As a result, short-latency saccades typically do not compensate for smooth eye displacements in darkness (Blohm et al. 2005b), whereas long-latency saccades almost fully compensate (Blohm et al. 2005b). For medium latency saccades, there is a partial compensation of the smooth eye displacement. These findings could be explained by a delayed integration of the smooth pursuit command by the saccadic system (Blohm et al. 2003, 2006).

Not much is known about this mechanism in head-unrestrained conditions. It has been shown that saccades can compensate for head rotations (Medendorp et al. 2002a,b) while maintaining fixation. Herter and Guitton (1998) have also shown that saccades to targets memorized before visually driven head-unrestrained pursuit are accurate. It remains unknown how spatial constancy is achieved for targets presented during ongoing head-unrestrained smooth pursuit eye movements. This is not a trivial extension of previous work on spatial constancy during smooth pursuit (Blohm et al. 2003, 2005a,b, 2006; Herter and Guitton 1998; McKenzie and Lisberger 1986; Schlag et al. 1990) because adding the head motor system also introduces interactions with the vestibuloocular reflex (VOR) (Angelaki and Cullen 2008; Barnes 1993). As a consequence, several questions arise. First, it remains unknown to what extent the displacements of the head during the saccadic latency period are taken into account in the compensation for head-unrestrained pursuit. Second, what is the time course of this compensation during head-unrestrained pursuit and which factors might it depend on? Third, what is the influence of the VOR on this process?

The VOR acts as a stabilization system for vision during the perturbations induced by head movements. During head-unrestrained eye movements, this is a counterproductive mechanism that needs to be suppressed or cancelled out by an additional oculomotor command (Barnes 1993). VOR cancellation is present during eye–head tracking (see, e.g., Lanman et

Address for reprint requests and other correspondence: P. Lefèvre, CESAME, Université catholique de Louvain, 1348 Louvain-la-Neuve, Belgium (E-mail: philippe.lefevre@uclouvain.be).

al. 1978). Lefèvre et al. (1992) showed that the VOR is suppressed as soon as the gaze saccade starts and that the VOR gain increases progressively before the end of the saccade. Using electrophysiological recordings of the vestibular nuclei, Roy and Cullen (2002, 2004) showed that the firing rate of vestibular nuclei neurons is attenuated when the discharge of neck proprioceptors matches the expected effect of the neck command during active head movements. Therefore we expect a reduction of the apparent VOR gain during head-free smooth pursuit; however, how large this reduction might be and how it might depend on the head movement frequency remains unknown.

To investigate how the saccadic system keeps track of head-unrestrained smooth eye displacements in darkness, we designed a head-unrestrained version of our previous two-dimensional (2D) tracking experiment (Blohm et al. 2003, 2005b). By briefly presenting a visual target during ongoing eye and head pursuit and asking subjects to orient toward the memorized location of this target, we were able to address how spatial constancy was obtained across movements of both effectors. We here show how the compensation for eye and head movements depends on the relative contribution of the eyes and head to the overall smooth gaze displacement during the saccadic latency period. In addition, we estimate an interval for plausible values of the VOR gain dependence on the head movement frequency during the orientation process in darkness.

METHODS

Eight human subjects (four male, four female, ages ranging from 22 to 32 yr) without any known oculomotor abnormalities participated in this experiment after giving informed consent. Three subjects (EM, LA, and GA) were completely naïve to oculomotor research, three subjects (CO, GL, and SC) were knowledgeable about general oculomotor studies, and two subjects (DP and GB) were knowledgeable about the purpose of the study. All procedures were approved by the Université catholique de Louvain ethics committee, in compliance with the Declaration of Helsinki.

Experimental setup

Subjects sat 1 m in front of a translucent tangent screen in a completely dark room. The screen spanned ±40° of their horizontal and vertical visual field. A green and a red laser spot (0.2° diameter) were back-projected onto the screen. Target position was controlled by mirror-galvanometers (GSI Lumonics, Billerica, MA) at 1 kHz via an embedded real-time computer (PXI-8186 RT, National Instruments, Austin, TX) running LabVIEW (National Instruments). Horizontal and vertical eye movements were recorded at 200 Hz by a Chronos head-mounted video eye tracker (Chronos Vision, Berlin). To keep a good accuracy during the video recording of the eye position, it is important to reduce any relative movement between the position of the eye and the Chronos helmet. To that goal, a bite bar was mounted onto the Chronos frame to prevent any slippage of the helmet during head movements. The subject's head was free to move. Head position was computed from the position of a set of six infrared light-emitting diodes (IREDs) mounted onto the Chronos helmet. IRED position was sampled at 200 Hz by two three-dimensional (3D) optical infrared cameras (Codamotion system, Charnwood Dynamics, Leicestershire, UK).

Paradigm

A recording session was composed of eight blocks of 25 trials. Each trial started with a fixation of a red target at the center of the screen for 500 ms. Then the target performed movements along a randomly oriented straight line with a sinusoidal velocity at a random frequency ([0.6 . . . 1.2] Hz) and random amplitude ([20 . . . 25] deg) over a random duration ([3,000 . . . 3,750] ms). For all randomizations, we sampled in a continuous fashion (uniform distribution) between the specified boundaries. Around the end of the red target motion, a green target was briefly presented (duration: 10 ms) and hereafter will be referred to as the "flash." The flashed target was located inside a virtual annular surface and could appear at a random radius ([15 . . . 30] deg) and at a random orientation ([0 . . . 360] deg) with respect to the pursuit target. The flash could be presented either at the same time, before, or after the extinction of the pursuit target. The probability of occurrence of these three conditions was equal. The duration between flash presentation and pursuit extinction was randomly selected from the following list of possible values: [200, 175, 150, 125, 100, 75, 50, 25, 0, −100, −200, −300, −400, −500, −600, −700, −800] ms. This resulted in a gap condition (Fig. 1*A*), a no gap no overlap (NGNO) condition (Fig. 1*B*), and an overlap condition (Fig. 1*C*). We used these different conditions to increase both the range of observed gaze saccade latencies and head movement amplitudes during the saccade latency period following the presentation of the flash (see following text).

During the pursuit part of the protocol, subjects were asked to track the red target actively with both their eyes and head. They were asked to reorient their gaze to the memorized position of the flash as soon as they saw the flash and to maintain gaze on this memorized location until a second end-of-trial target appeared for 500 ms at the center of the screen. The orientation period after the flash presentation lasted for ≥1 s so that the overall duration of all trials was 6 s.

Data calibration

We performed three calibration blocks during an experimental session: one at the start of the experiment, one midway through the session, and one after the last experimental block of trials. Calibration was necessary to reconstruct gaze (i.e., eye orientation relative to an inertial reference frame) from eye-in-head orientation measurements taken by the Chronos eye tracker and head-in-space orientation obtained through the IRED positions. Each calibration was composed of five series of five successive fixation targets (each fixation lasted

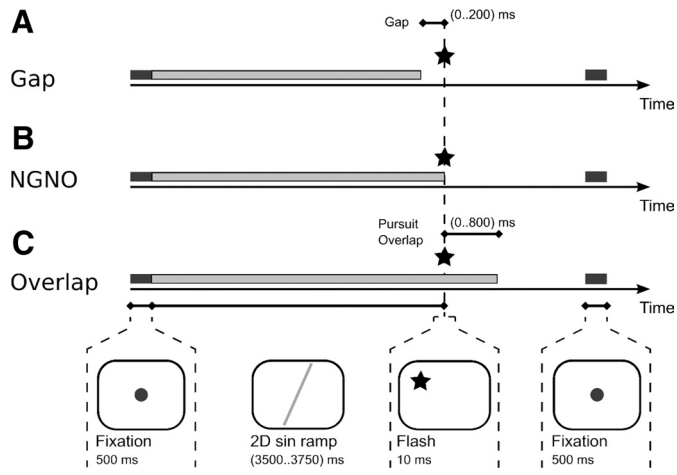

FIG. 1. Experimental protocol. The trial starts with a 500-ms fixation at the center of the screen. Then a red pursuit target with a random sinusoidal velocity along a randomly oriented ramp with random amplitude is presented for a random duration. Afterward, a green target is flashed (duration: 10 ms) at a random position. *A*: gap. The pursuit target is off before the flash presentation for a random duration ≤200 ms. *B*: No Gap No Overlap (NGNO). The pursuit target is off when the flash is presented. *C*: overlap. The pursuit target is still on for a duration ≤800 ms after the flash presentation. Trial ends with a center fixation for 500 ms.

2 s). Subjects were asked to maintain their head position during a fixation series and to move it to a new position between two series.

This calibration sequence allowed determination of the IRED positions for the primary upright straight-ahead head position. All head movements were computed as the angular difference from this primary orientation. Next, we reconstructed gaze from the eye-tracker and head-orientation data using a previously described method (Ronsse et al. 2007). Briefly, this method computes the exact relationship between eye-centered, head-centered, and inertial reference frames to estimate a 3D gaze orientation vector from eye-in-head and head-in-space positions and orientations. This method also required determining the relative position of the eyes with respect to the head markers, which we measured by holding an IRED onto the closed eyeball. Finally we transformed eye-in-head, head-in-space, and gaze-in-space orientations into the target reference frame (as if all centers of rotation align), which resulted in the gaze being the sum of eye and head orientations.

Data analysis

The IRED and eye positions were stored on a computer hard drive for off-line analysis. Matlab (The MathWorks, Natick, MA) was used to implement analysis algorithms. Recorded data were low-pass filtered (cutoff frequency: 50 Hz) using a zero-phase digital filter (autoregressive, forward–backward filter). Velocity and acceleration were derived from position using a central difference algorithm on a ±10-ms window. Data were rotated with respect to pursuit target direction sampled either at flash time for NGNO and overlap conditions or at pursuit target disappearance for the gap condition. This rotation induced a new coordinate system; the movement was decomposed into direction parallel to pursuit (X-axis in text and figures) and direction orthogonal to pursuit (Y-axis in text and figures).

Gaze saccade detection was based on a Kalman filter (Sauter et al. 1991) combined with a generalized likelihood ratio (GLR) fault-detection algorithm (Basseville and Nikiforov 1993). Onset and offset of a detected gaze saccade were computed with a traditional acceleration threshold (750°/s^2) on the eye-in-head signal (de Brouwer et al. 2002a,b). Every trial was visually inspected; the acceleration threshold was decreased to 500°/s^2 if a saccade was not automatically detected. All trials were aligned to flash presentation.

As part of our analyses, we computed the absolute and relative latency of every saccade within a trial. Absolute latency of a saccade was defined as the time between the flash presentation and gaze saccade onset. Relative saccade latency was defined as the time between onsets of two successive saccades. To estimate the latency distribution, we used a linear approach to threshold with ergodic rate (LATER) model (Carpenter and Williams 1995). The LATER model assumes both a linear rate of rise of a decision signal to a threshold value and that the rate of rise has a Gaussian distribution. To obtain the parameters of the LATER model, we fitted a recinormal (inverse-Gaussian) distribution on our data

$$\mathrm{f}(\mathrm{Lat}, \mu, \gamma) = \sqrt{\frac{\gamma}{2 \times \pi \times \mathrm{Lat}^3}}\, e^{-[\gamma(\mathrm{Lat}-\mu)^2]/[2\times\mathrm{Lat}\times\mu^2]} \quad (1)$$

This distribution is characterized by a mean μ and SD $\sigma = \sqrt{\mu^3/\gamma}$.

We also define the smooth gaze displacement (SGD) as the gaze movement after removing gaze saccades. To remove a gaze saccade, the velocity from 20 ms before a gaze saccade onset up to 20 ms after the gaze saccade offset was replaced by a linear interpolation (for a detailed procedure see de Brouwer et al. 2001). Through this procedure of saccade removal, we assume that the gaze displacement is the sum of saccadic and smooth tracking commands because this has been shown during head-restrained smooth pursuit (de Brouwer et al. 2001, 2002b). Smooth head displacement (SHD) was defined as the head displacement during the experiment. Then we defined smooth eye displacement (SED) as SED = SGD − SHD. We computed head contribution (HC) to the gaze displacement as HC = SHD/SGD. Equivalently, eye-in-head contribution (EC) to the gaze displacement was computed as EC = SED/SGD. Straightforward computations give EC = 1 − HC. An EC = 0 means that SGD was entirely realized by head displacement. In contrast, an EC = 1 indicates that SGD was completely comprised of eye displacement (it can be seen as a head-restrained situation). An EC of <0 or >1, respectively, means that the head was moving faster than the gaze or in the opposite direction of the gaze (the same kind of reasoning applies to HC).

To characterize the head movement during the pursuit part of the paradigm, we evaluated the frequency of head movement. First, we selected the head movement preceding flash presentation for a duration equivalent to 1.2 periods of target oscillation. We then determined the head movement frequency as the maximum of the frequency spectrum after fast Fourier transformation. Thus we assume that the head oscillation frequency was stable during this elapsed time. To test this assumption, we divided the selected head movement in two subparts and computed for each part the head oscillation frequency. We then performed a two-tailed *t*-test and found that the two distributions had an equivalent mean [two-tailed *t*-test, $t(2780,2780) = 0.1999$, $P = 0.842$]. Those results validated our hypothesis of constant head oscillation frequency.

Compensation

To quantify the effect of SGD on the final orientation error, we computed a compensation index (CI) describing how much of the smooth gaze displacement occurring after the flash was accounted for by the saccadic system at the end of the orientation process. To do so, we defined PE as the remaining position error at the end of an orienting gaze saccade and SGD as the smooth gaze displacement between flash presentation and the onset of the considered orientation saccade. Normalization of the data resulted in SGD mainly in the X direction (direction parallel to pursuit); therefore we assume that the SGD along the Y direction was negligible compared with SGD along the X direction. Thus we analyzed only the X component. We measured SGD at the saccade onset because we were interested in how much a given saccade would compensate for SGD that had occurred before execution of the saccade. Assuming that all pure position error at the moment of the flash is perfectly accounted for by the saccadic system (de Brouwer et al. 2002b), one can then write the position error as

$$\mathrm{PE} = \mathrm{SGD} - \mathrm{CI} \times \mathrm{SGD} \quad (2)$$

Solving for the CI then results in

$$\mathrm{CI} = \frac{\mathrm{SGD} - \mathrm{PE}}{\mathrm{SGD}} \quad (3)$$

When PE is equal (both the sign and the magnitude) to SGD, the saccade did not compensate for SGD and CI = 0. When PE = 0, the compensation is perfect, i.e., CI = 1. An overcompensation of the saccade would result in PE having the opposite sign as SGD and CI >1. Figure 2*A* shows a graphical representation of the parameters involved in the computation of the global compensation index.

However, *Eqs. 2* and *3* only describe the overall compensation for gaze displacement but do not allow inferring the individual compensation indices for smooth eye (SED) and head (SHD) displacements. Using SGD = SHD + SED, we can now write

$$\mathrm{PE} = \mathrm{SGD} - \mathrm{CI}^{\mathrm{E}} \times \mathrm{SED} - \mathrm{CI}^{\mathrm{H}} \times \mathrm{SHD} \quad (4)$$

With EC = SED/SGD, HC = SHD/SGD, and HC = 1 − EC, *Eq. 4* can be modified to explicitly include the eye and head compensation indices (CI^{E} and CI^{H}, respectively) as follows

$$\frac{\mathrm{SGD} - \mathrm{PE}}{\mathrm{SGD}} = \mathrm{CI} = \mathrm{CI}^{\mathrm{E}} \times \mathrm{EC} + \mathrm{CI}^{\mathrm{H}} \times (1 - \mathrm{EC}) \quad (5)$$

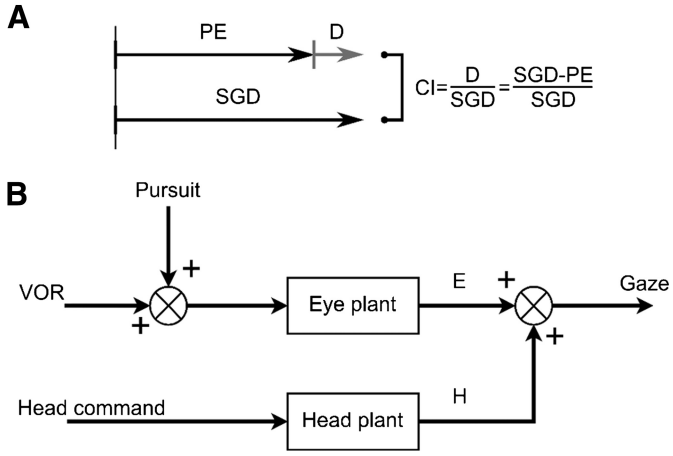

FIG. 2. *A*: representation of the parameters involved in the computation of the global compensation index. PE corresponds to the position error. SGD represents the smooth gaze displacement. D is the difference between SGD and PE. *B*: hypothetical model of the compensation process during gaze shift latency. VOR corresponds to the integrated vestibuloocular signal coming from the semicircular canals, proportional to head displacement. Pursuit corresponds to eye command signal. E corresponds to the measured eye-in-head displacement during the latency. H corresponds to the measured head displacement during the latency. Thus the gaze is a sum of the pursuit, the VOR, and the head displacement.

Furthermore, we can separate the smooth eye displacement (SED) into a vestibuloocular reflex (VOR) component and a smooth pursuit displacement (SPD), i.e., SED = SPD + VOR. This is shown in Fig. 2*B*. At the level of the oculomotor neurons, the command sent to the eye plant is composed of the VOR and SPD while the head plant receives a single input, the SHD. We can also implement the finding that the VOR depends on head movement, i.e., VOR = $-g(f_H) \times$ SHD, where $g(f_H)$ is the VOR gain depending on the head movement frequency f_H. It is well known that the VOR gain varies as a function of a number of parameters (for a review see Barnes 1993). Nevertheless, for the sake of this study, we considered that the VOR gain can be approximated by an average value over the first saccade latency period. This mean value depends on the head oscillation frequency of individual trials (see Fig. 10 of Barnes 1993). Using these considerations and *Eq. 4*, we can now write

$$PE = SGD - CI^P \times EC \times SGD - [(CI^V - CI^P) \times g(f_H) + CI^H] \times (1 - EC) \times SGD \quad (6)$$

$$CI = [CI^P - (CI^P - CI^V) \times g(f_H) - CI^H] \times EC + [(CI^P - CI^V) \times g(f_H) + CI^H] \quad (7)$$

Equation 7 gives a more detailed expression of the evolution of the overall compensation index as a function of the different components (pursuit, VOR, and head) of the SGD. The complete mathematical developments to obtain *Eq. 7* are given in the APPENDIX.

Collected data set

We collected a total of 6,533 trials, of which 2,783 were valid (~42.6%). Trials were removed from the analysis if a saccade occurred during an interval of [−50 . . . 50] ms around the flash presentation (39.6% trials removed). We also removed trials for which the final gaze position error had a magnitude either >16° or larger than the error at flash time (13.4% trials removed). Those cases corresponded to situations in which flash localization was erroneous or ambiguous. Finally, we removed "catch-up trials," where the first saccade after the presentation of the flash was directed toward the pursuit target (4.4% trials removed) instead of the flash. Every trial was visually inspected and removed if it did not comply with the above-cited validity criteria. Among valid trials, 1,137 were gap trials (~41%), 910 were no gap no overlap (NGNO) trials (~33%), and 736 were overlap trials (~26%).

RESULTS

The aim of this study was to investigate how the saccadic system compensated for smooth gaze displacements in a head-unrestrained condition and whether this compensation differed between the smooth pursuit, head, and VOR components of the smooth gaze displacement. Therefore we will first show typical trials and analyze orienting saccade latencies. We also showed how the compensation for smooth eye and head displacements depends on saccade latency and the relative contribution of the eye movement to the total smooth gaze displacement. Finally, we estimated an upper limit for the rate of change of the VOR gain with different head movement frequencies during the orientation process.

Typical trials

Figure 3 shows a short-latency gap trial (gap duration: 200 ms) in which the first orienting saccade had a latency of 100 ms. Figure 3*A* shows an X–Y plot of target and gaze trajectories in space, starting 400 ms before the flash presentation (the star represents the location of the 10-ms flash, whereas the dot represents gaze position at the moment of flash presentation) until 800 ms after the occurrence of the flash. Gaze (thin dark gray line) pursued the oscillating target (0.7 Hz, 29° amplitude, light gray line) to the right in Fig. 3*A* and two orienting gaze saccades toward the memorized location of the flash were generated (bold gray lines). Figure 3*B* shows the individual components of gaze, eye, and head position as a function of time for the same trial. Figure 3*C* shows a detailed view of the gaze displacement after the flash. As can be seen, gaze continued to track the now invisible red target during the gap (gray boxes) and continued moving for about 100 ms after the flash presentation. During the latency of the first gaze saccade, smooth gaze displacement (SGD) along the direction normal to pursuit was negligible (−0.84°) compared with SGD parallel to pursuit (8.55°, SGD label on Fig. 3*C*) and the eye contributed only minimally (EC: 8.7%). As can be observed in Fig. 3*A*, the direction of the first orienting gaze saccade was approximately parallel to the position error at flash presentation. Because this saccade obviously did not account for SGD during the latency period, the position error was still large (PE = 6.01°, PE label on Fig. 3*C*) at the end of the first gaze saccade. Therefore the system executed a second corrective gaze saccade (with a latency of 310 ms) toward the remembered flash position, resulting in a final orientation error of PE = −3.32°. Importantly, this corrective saccade could not rely on visual information about the SGD due to darkness and thus had to result from some mechanism that internally monitored the SGD.

A different behavior was observed in our second typical example, as is shown in Fig. 4 (same conventions as those in Fig. 3 apply). This NGNO trial shows a long-latency (385 ms) response to a flash presented after gaze pursuit (amplitude = 21°, frequency = 0.64 Hz), where SGD before the first saccade was 16.6° (EC = 14.9%). This saccade resulted in a position error of 1.03° and a second, corrective saccade (with a latency

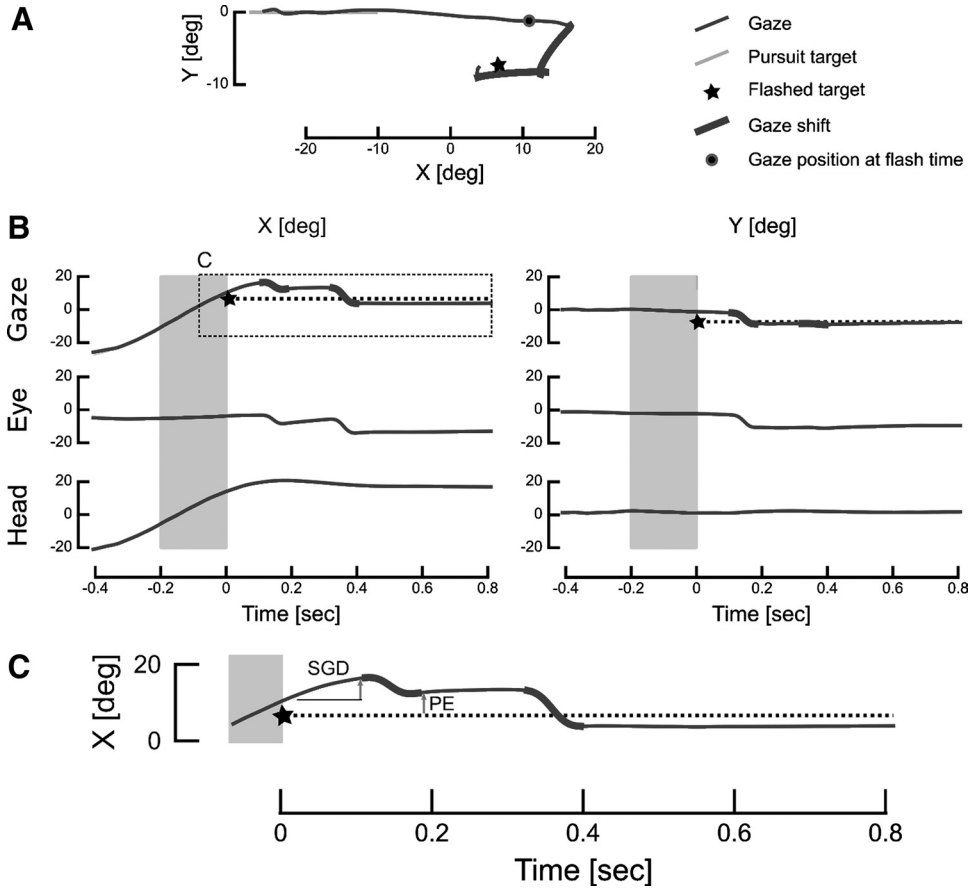

FIG. 3. Typical normalized short latency trial. X corresponds to the direction parallel to pursuit; Y represents the direction normal to pursuit. *A*: spatial representation of the normalized gaze and target position. *B*, *left column* represents X evolution as a function of time for either gaze, eye-in-head, or head (depending on rows); *right column* represents Y evolution for the same signals. Time origin is set at the flash appearance. The dashed line in the gaze row represents the flash position. Shaded boxes represent gap period (duration: 200 ms). *C*: detailed representation of X evolution as a function of time. Relevant gaze shifts are represented with bold lines on *A*, *B*, and *C*.

of 590 ms) brought the gaze to a final position error of −2.53°. Compared with the short-latency trial in Fig. 3, the first saccade of this trial immediately corrected for the SGDs that occurred during the latency period and thus the saccade was quite accurate (compare PE amplitudes between Figs. 3 and 4).

As explained in METHODS, the SGD along a direction orthogonal to the pursuit target direction is negligible compared with the component along the pursuit target direction (mean SGD_X = 7.75°, mean SGD_Y = 0.83°).

Latency distribution

As can be readily observed from the typical trials, and in agreement with previous findings (Blohm et al. 2003, 2005b), the saccadic latency has an important role in determining the accuracy of the gaze position. Therefore we first set out to characterize saccade latencies. Figure 5*A*, shows the distribution of absolute latencies (time between flash appearance and gaze saccade onset) of the three first gaze saccades for all subjects and all conditions pooled together (first saccade: □, second saccade: ▨, third saccade: ■). The relative latency (with respect to flash presentation for the first saccade and with respect to the previous saccade onset for successive saccades) is shown in Fig. 5*B*. To further characterize the relative latency distribution, we fitted a LATER model (see METHODS) on each distribution. The means (±95% confidence intervals) of these distributions for the first, second, and third saccades are 254 ± 7 ms (CI: 101 ± 1 ms), 298 ± 10 ms (CI: 125 ± 1 ms), and 298 ± 21 ms (CI: 145 ± 2 ms), respectively. Table 1 shows these parameters for each subject individually (note that we did not fit a LATER model on data sets with <40 samples). Statistical analysis showed that relative saccade latencies differed between the first and second saccades (two-sided Kolmogorov–Smirnov test [KS], $P < 0.001$) but not between the second and third saccades (two-sided KS, $P = 0.085$).

To evaluate differences in latency distribution due to variations in flash presentation conditions, we evaluated LATER models for the latency distributions of the first gaze saccades separately for the gap condition (mean = 205 ± 7 ms, SD = 76 ± 1 ms), the NGNO condition (mean = 263 ± 8 ms, SD = 83 ± 3 ms), and the overlap condition (mean = 299 ± 13 ms, SD = 95 ± 4 ms). These results showed that the three flash presentation conditions had an influence on the observed latency of the first gaze saccade. There was a significant increase in latency between the gap and the NGNO conditions (two-sided KS, $P < 0.001$) and between the NGNO and the overlap conditions (two-sided KS, $P < 0.001$), results that are in agreement with head-restrained findings obtained by Krauzlis and Miles (1996). The goal of our experimental paradigm—to obtain a large range for first saccade latencies—was thus achieved.

Eye contribution distribution

Besides saccade latency, another important factor that might influence the compensation for smooth gaze displacements is the eye contribution (EC). EC was chosen as a parameter because, as will be shown later, it is an independent parameter with respect to the latency (which is not the case for SED and SHD). Therefore we analyzed to what extent the eyes and head

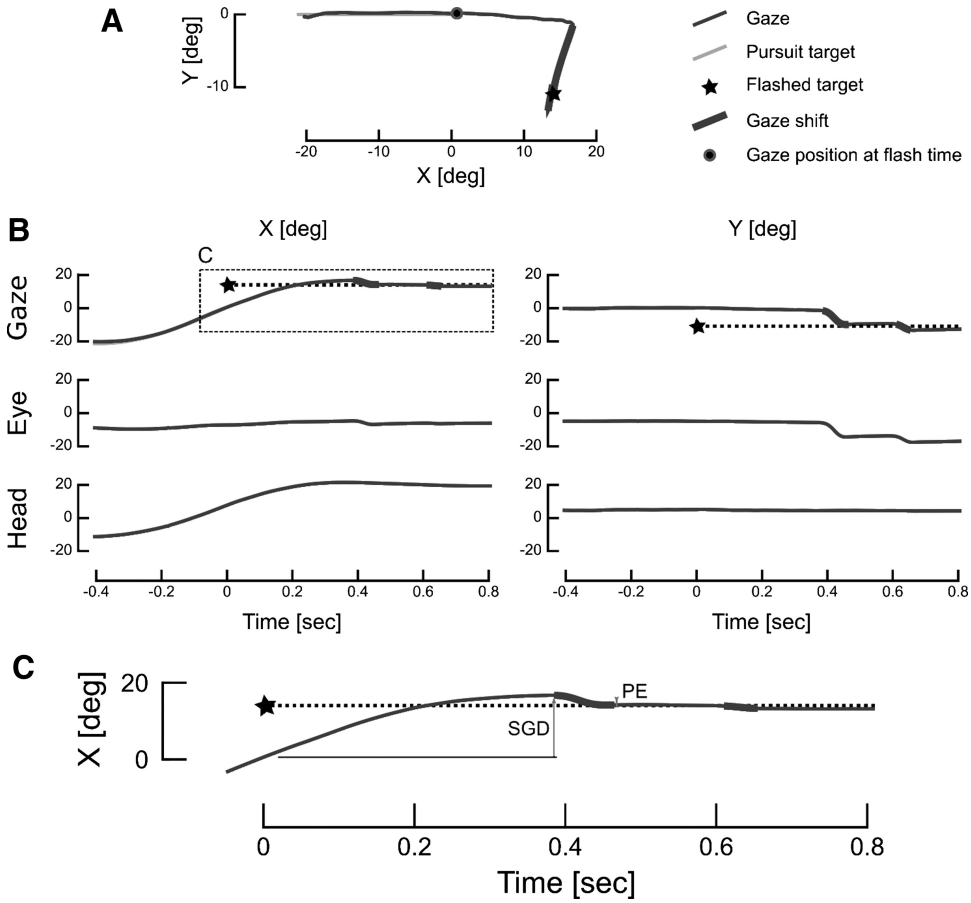

FIG. 4. Long latency trial. Same conventions as in Fig. 3. *A*: spatial representation. *B*, *left column* represents X evolution as a function of time for gaze, eye-in-head, or head. *Right column* represents Y evolution as a function of time for the same signals. *C*: detailed representation of X evolution as a function of time.

contributed to the gaze displacement during the latency period of the saccades. Figure 6 shows SGD as a function of SED (Fig. 6*A*) and SHD (Fig. 6*B*) for trials containing a single saccade. EC is color-coded in Fig. 6. Given a certain SED (SHD), the range of associated SGD values can be determined from these graphs. The variability of associated SGD values in these data is important because it allows us to analyze compensation for smooth eye and head displacements separately, despite their obvious correlation. This can be observed from the arrows on Fig. 6*A*, which represent the evolution of EC. Because EC = SED/SGD, when SGD approaches zero, eye contribution approaches ±infinity. To avoid this issue, we removed trials with $\| \text{SGD} \| < 1°$ (see *insets* in Fig. 6, *A* and *B*), leaving 82% (1,305 trials) of first-saccade trials. That the contribution of the eye to a given SGD is not stereotypical is also apparent in Fig. 6*C*, where we present a histogram of ECs. This observation was crucial to allowing for the separate analyses of compensation for smooth eye and head movements during the latency period (see following text).

Compensation as a function of latency

Our typical trials depicted in Figs. 3 and 4 clearly show that the compensation for SGDs depends on saccade latency, as previously shown for head-restrained pursuit (Blohm et al. 2003, 2005b). To quantify the overall behavior for combined eye–head gaze displacements in our head-unrestrained data, we calculated a compensation index for SGD (see METHODS) and for up to three orientation saccades. We then separately plotted in Fig. 7 the mean compensation index as a function of absolute saccade latency (i.e., flash presentation time; grouped

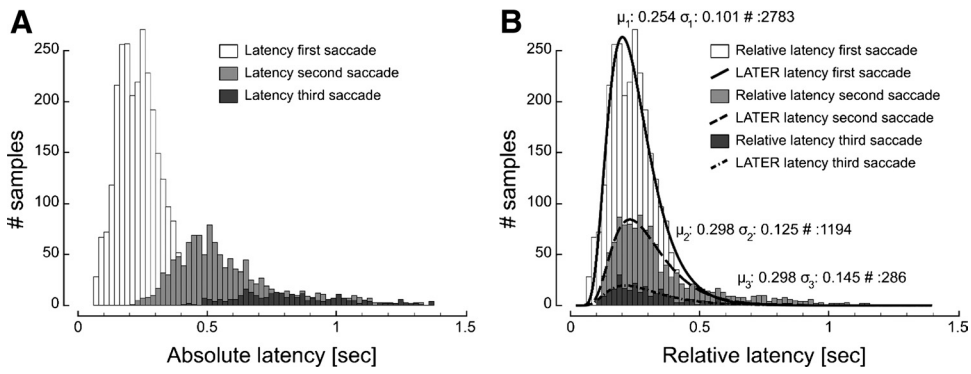

FIG. 5. Latency distribution. *A*: absolute saccade latency distribution for the 3 first saccades. First saccade distribution includes first saccades for trials with 1, 2, or 3 saccades; second saccade distribution includes second saccades for trials with 2 or 3 saccades; and third saccade distribution includes third saccades for trials with 3 saccades. *B*: relative saccade latency distribution, with the same color convention and for the same trials as *A*. LATER models were fitted on relative latency distributions. Maximums of recinormal vary from 254 to 298 ms.

TABLE 1. *LATER model parameters on gaze saccade relative latency for every subject*

	First Gaze Saccade			Second Gaze Saccade			Third Gaze Saccade		
Subject	Number of Trials	Mean, ms	SD, ms	Number of Trials	Mean, ms	SD, ms	Number of Trials	Mean, ms	SD, ms
CO	378	178 ± 4	51 ± 2	146	339 ± 43	190 ± 11	15	—	—
DP	398	265 ± 8	58 ± 5	195	381 ± 32	157 ± 4	65	252 ± 20	83 ± 8
EM	410	318 ± 12	110 ± 3	186	263 ± 13	94 ± 3	27	—	—
GA	294	274 ± 7	82 ± 3	69	283 ± 13	81 ± 6	9	—	—
GB	245	242 ± 8	64 ± 4	192	229 ± 9	65 ± 4	89	254 ± 26	125 ± 2
GL	358	270 ± 11	87 ± 4	205	284 ± 15	115 ± 1	41	347 ± 65	183 ± 10
LA	437	213 ± 7	62 ± 3	96	296 ± 25	141 ± 1	11	—	—
SC	263	253 ± 27	142 ± 7	105	323 ± 15	81 ± 8	29	—	—
ALL	2,783	254 ± 7	101 ± 1	1,194	298 ± 10	125 ± 1	286	298 ± 21	145 ± 2

Values are means ± confidence interval at 95%. We did not fit a LATER model on data sets with >40 trials.

in 50-ms bins) for each saccade individually (Fig. 7*A*) and for the last orientation saccade of the trial only (Fig. 7*B*).

Figure 7*A* shows that for the first gaze saccade, the compensation increased with latency. For latencies up to around 200 ms, the compensation was not statistically >0 [upper tail *t*-test, $t(166) = -1.9746$, $P = 0.975$ at 100 ms; $t(506) = -3.73$, $P > 0.999$ at 150 ms], whereas the compensation index reached significance for latencies ≥200 ms [mean CI values for all first saccade latencies ≥200 ms = 0.39 ± 0.03; upper tail *t*-test; $t(1,725) = 25.76$, $P < 0.001$]. Because after the first gaze saccade the spatial error generally remained large, we often observed a second (~43% of the trials) or even third (~10% of the trials) corrective saccade. Across the latencies of the second saccade, we continued to observe an increase in CI (CI = 0.36 ± 0.22 at 300 ms, CI = 0.58 ± 0.12 at 400 ms). At this point, CI reached a plateau value (mean CI = 0.64 ± 0.05 for second saccade with latency >400 ms, mean CI = 0.57 ± 0.15 for third saccade) and we did not observe any further statistically significant change of CI with saccade latency [two-tailed *t*-test, $t(615) = 29.67$, $P < 0.001$]. Note that the transition between the CI evolution curves for the three saccades is surprisingly smooth, which suggests that it is not the number of saccades that determine the amount of SGD compensation but rather when the saccade was triggered relative to flash presentation.

Figure 7*A* represents the intermediate stages of the compensatory mechanism for all saccades individually. To study the global orientation process, we computed CI for the last saccade of a trial ("final compensation") and plotted it as a function of saccade latency in Fig. 7*B*, similarly to Fig. 7*A*. As can be observed, the shape of this curve is very similar to the CI of the individual saccades. As in Fig. 7*A*, the compensation in Fig. 7*B* starts to be significantly >0 only for latencies >150 ms [CI = 0.28 ± 0.09 at 200 ms; upper tail *t*-test, $t(324) = 6.4$, $P < 0.001$]. With an increase in latency, we observed a significant increase in CI, up to latencies of 300 ms [CI = 0.28 ± 0.09 at 200 ms, CI = 0.56 ± 0.06 at 300 ms; $t(324,297) = -5.016$, $P < 0.001$]. At this point, the global compensation reaches a plateau and we did not observe any further significant changes [mean CI = 0.62 ± 0.02, two-tailed *t*-test, $t(1,330) = 50.53$, $P < 0.001$].

To evaluate the individual performances of our subject, we computed the mean value of the final compensation index for absolute latencies >400 ms for every subject. The corresponding values are presented in Table 2.

To summarize, we have qualitatively reproduced previous findings from head-restrained situations (Blohm et al. 2003, 2005b, 2006) and generalized them to head-unrestrained smooth pursuit. Figure 7 also shows that there is a continuous transition between two extreme behaviors in our typical trials

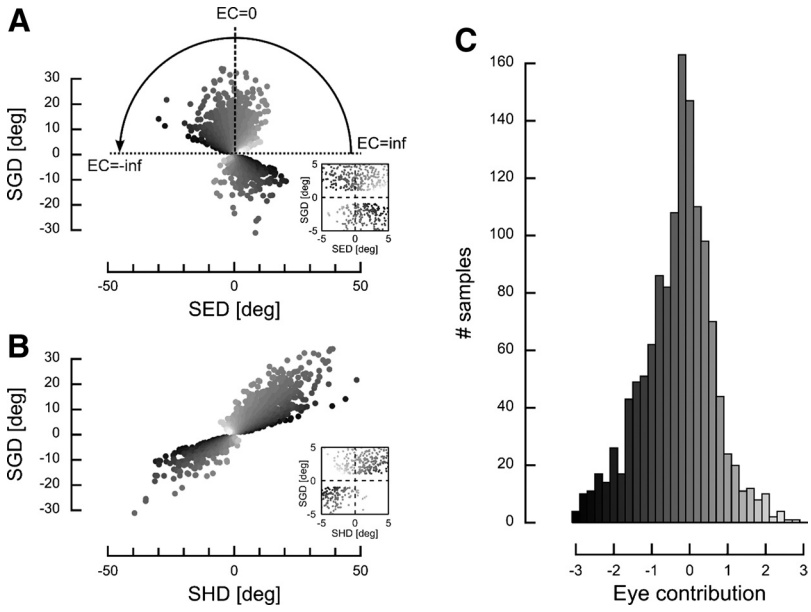

FIG. 6. Eye contribution distribution. *A*: smooth gaze displacement (SGD) as a function of smooth eye displacement (SED) for single-saccade trials. *B*: SGD as a function of smooth head displacement (SHD) for single-saccade trials. *Insets* on *A* and *B* represent a zoomed portion of their corresponding panels. Those *insets* show that we removed trials with absolute SGD amplitude <1°. *C*: eye contribution (EC = SED/SGD) distribution for single saccade trials. We represented data with $-3 < EC < 3$, which included 94% of the single-saccade trials. On each panel, when EC is small, the data representation is darker and when EC is large, the data representation is lighter. The arrow on *A* represents EC evolution from −infinity to +infinity (from light to dark).

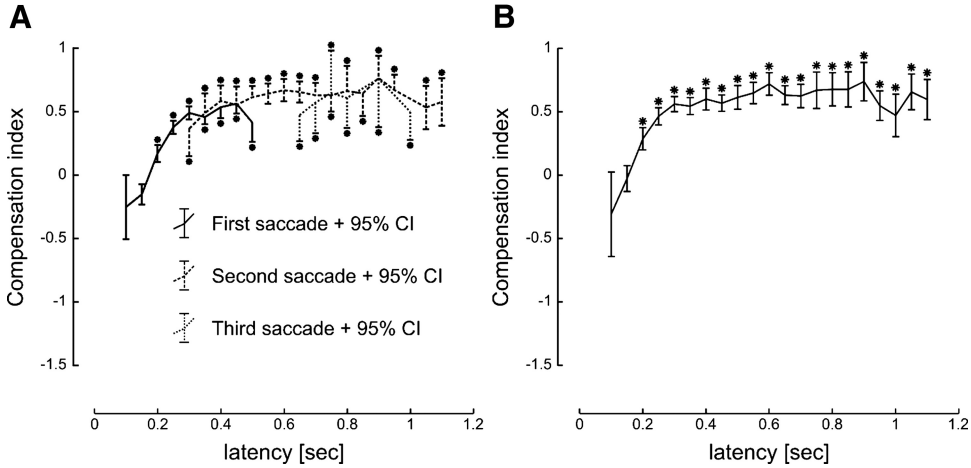

FIG. 7. Compensation as a function of absolute latency. *A*: evolution of the compensation index (CI = 1 − PE/SGD) as a function of absolute latency for the third first saccades of a trial. First saccade curve includes trials with 1, 2, or 3 saccades; second saccade curve includes trials with 2 or 3 saccades; and third saccade curve includes trials with 3 saccades. Error bars represents 95% confidence intervals. Stars on error bars represent bins with a compensation index significantly greater than zero ($P < 0.05$). *B*: evolution of the final compensation index (compensation index for the last saccade of a trial) as a function of absolute latency. Stars on error bars represent bins with a compensation index significantly greater than zero ($P < 0.05$).

(Figs. 3 and 4), apparently implementing the speed–accuracy trade-off and the existence of a continuous compensatory mechanism previously suggested (Blohm et al. 2005b). After this necessary verification, we next analyzed the compensatory mechanism for the eye- and head-related components of the SGD separately (see following section).

Eye and head compensation

Up to this point, we have shown that the global gaze compensation mechanism is similar during head-unrestrained pursuit and head-restrained pursuit, as previously reported (Blohm et al. 2003, 2005b). In this section, we will decompose the SGD into its respective eye- and head-movement components to investigate potential differences in compensation for smooth eye displacements (SEDs) and smooth head displacements (SHDs).

To analyze the potential differences between compensation for smooth eye and head displacements, we represented the compensation index as a function of eye contribution (EC; see METHODS for definition) on Fig. 8*A* for the same subset of trials as in Fig. 6 (single saccade trial, $\|\text{SGD}\| > 1°$). The rationale behind this analysis is that if smooth eye and head displacements are equally accounted for, then the correlation between CI and EC should be zero. In contrast, any nonzero correlation means that there are differences in the compensation for SED and SHD. A linear regression analysis provided the following result

$$\text{CI} = (0.25 \pm 0.03) \times \text{EC} + (0.53 \pm 0.03)$$

$$\text{vaf} = 0.42, P < 0.001 \qquad (8)$$

The relationship between CI and EC clearly points toward a difference in the mechanisms compensating for SED and SHD. When analyzing subjects individually, we found that the slope of the regression varies in a range between 0.1229 and 0.48.

To ensure that this observation was not due to a side effect of the saccade latency (i.e., the longer the latency, the smaller the EC), we performed several control analyses. First, we subdivided our data into several EC bins and drew the evolution of CI with saccade latency (Fig. 8*B*). Figure 8, *B1–B3* shows representative plots of this relationship for EC = −1.4 (Fig. 8*B1*), EC = 0 (Fig. 8*B2*), and EC = 0.6 (Fig. 8*B3*). Figure 8*B* shows that for each EC bin, CI evolves similarly to what we have observed in Fig. 7 (the longer the latency, the greater the compensation). Nevertheless, the mean value of compensation is less important for smaller values of EC (Fig. 8*B1*: CI = −0.02 ± 0.25) than for larger values of EC (Fig. 8*B3*: CI = 0.78 ± 0.18).

Next, we tested the independence between EC and latency. To do so, we used a method proposed by Diks and Manzan (2002). This method uses a bootstrap procedure on the mutual information between EC and latency to test the null hypothesis that the two samples are independent. The test confirmed the independence hypothesis ($P > 0.73$), pointing toward latency having no effect on EC. We further tested whether the saccade latency distribution might change across bins of EC and thus induce a correlation between EC and CI. We therefore compared the latency distributions for each EC bin in Fig. 8*A*, but did not find any difference between latency distributions across the EC bins (2D KS test, $P > 0.05$), except for that in one comparison ($P = 0.0085$). Using the same method, we compared the global latency distribution with the latency distributions corresponding to each EC bin and did not find any differences ($P > 0.05$). Consequentially, we made sure that for each EC bin there was an equivalent range of saccade latencies. Taken together, these results suggest that there was an increase of CI with EC independent of saccade latency.

Once this independent effect of EC on CI was established, we could use *Eq. 5* to compute individual CIs for smooth eye and head movements from the parameters identified in *Eq. 8*. This resulted in $\text{CI}^{\text{E}} = 0.78 \pm 0.03$ and $\text{CI}^{\text{H}} = 0.53 \pm 0.03$. Therefore on average 78% of smooth eye movements and 53% of smooth head movements that occurred during the latency period of the saccade were compensated for by the saccadic

TABLE 2. *Mean final contribution for latencies >400 ms for each subject*

	Subject								
	CO	DP	EM	GA	GB	GL	LA	SC	ALL
Final compensation, %	75.9 ± 11	68 ± 5.8	53.3 ± 12.4	53.3 ± 2	37.4 ± 3	77.7 ± 11.6	17.6 ± 3	41.9 ± 6	62 ± 2

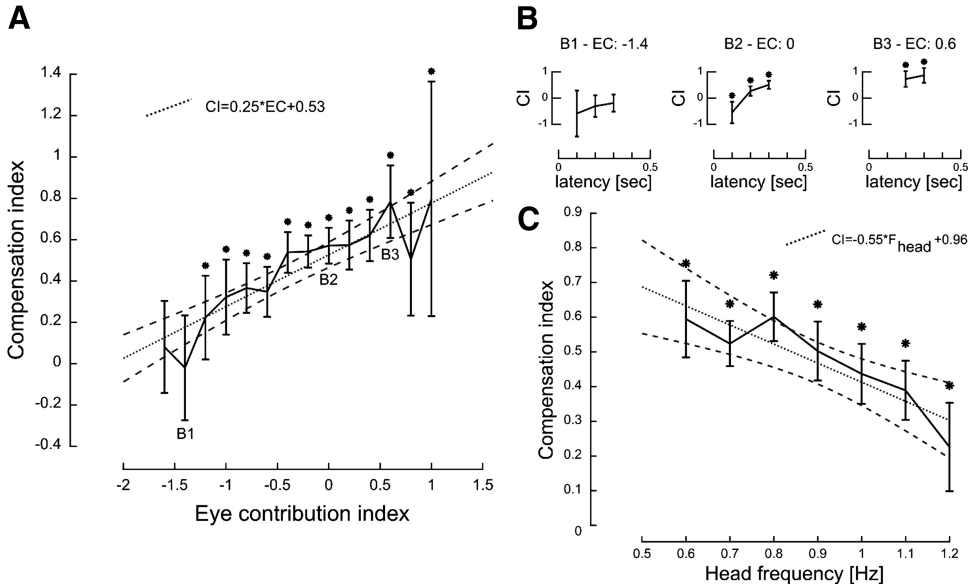

FIG. 8. Compensation as a function of eye contribution (EC) and head oscillation frequency (f_{head}). *A*: evolution of the compensation index (CI) as a function of EC. The dotted line represents a linear fit between CI and EC and dashed lines represent 95% confidence intervals of the fit. Stars on error bars represent bins with CI significantly greater than zero ($P < 0.05$). *B*: evolution of CI as a function of absolute latency for trials within an EC bin. *B1* corresponds to trials with $-1.5 < EC < -1.3$, *B2* corresponds to trials with $-0.1 < EC < 0.1$, and *B3* to trials with $0.5 < EC < 0.7$. Stars on error bars represent bins with CI significantly greater than zero ($P < 0.05$). *C*: CI evolution as a function of head oscillation frequency (f_{head}). The dotted line represents a linear fit between CI and f_{head} and dashed lines represent 95% confidence intervals of the fit.

system. As a result of the different CI values for eye and head, we can explain the linear relationship between CI and EC in Fig. 8 by the large range of different combinations of SED and SHD (and thus EC) in our data set.

A supplementary step to test the importance of EC in the evolution of CI was to test whether the addition of a supplementary parameter in a multiple regression analysis improved the quality of the fit. As can be observed in Fig. 7, the CI saturated for longer latencies. Conversely, Fig. 8*A* shows that the trend between EC and CI is well explained by a linear regression. Therefore we used a linear regression to describe the effect of EC on CI and added a nonlinear term to express the saturating effect of the latency on the CI. We then compared the regression with one parameter (saccade latency, *Eq. 9*) with the regression with two parameters (*Eq. 10*)

$$\mathrm{CI} = -e^{[-(1/0.059)\times \mathrm{Lat}+1.93]} + 0.48$$

$$\mathrm{vaf} = 0.46 \qquad (9)$$

$$\mathrm{CI} = -e^{[-(1/0.067)\times \mathrm{Lat}+1.76]} + 0.32 \times \mathrm{EC} + 0.67$$

$$\mathrm{vaf} = 0.75 \qquad (10)$$

Comparing the variance accounted for (vaf) of the fit, *Eqs. 9* and *10* show that the addition of supplementary parameters to the regression increased the quality of the fit. We performed an *F*-test and showed that the addition of a new parameter significantly increased the fit [one-sided *F*-test, $F(1,384,1,384) = 0.90$, $P < 0.05$]. This provides additional evidence that the eye contribution was an important parameter to explain the evolution of the compensation index.

As a final step, we attempted to further refine our analysis and divide SED into components resulting from an active smooth pursuit command and the vestibuloocular reflex (VOR). This is formalized in *Eq. 7* and now includes—aside from the three CIs relative to head, pursuit, and VOR—a head-movement frequency-dependent VOR gain term $g(f_H)$ (Barnes 1993). Unfortunately, we do not know the contribution of the VOR to SED and thus cannot directly evaluate the compensation for VOR. However, this is not the case for the pursuit compensation index. This can be directly seen when rewriting *Eq. 7* in the following form

$$\mathrm{CI} = A \times \mathrm{EC} + B$$

$$A = [\mathrm{CI}^P - (\mathrm{CI}^P - \mathrm{CI}^V) \times g(f_H) - \mathrm{CI}^H]$$

$$B = [(\mathrm{CI}^P - \mathrm{CI}^V) \times g(f_H) + \mathrm{CI}^H] \qquad (11)$$

Using *Eq. 11*, we could now directly evaluate the pursuit compensation index as $\mathrm{CI}^P = A + B$ using the parameters *A* and *B* from the regression in *Eq. 8*. This resulted in a value of $\mathrm{CI}^P = 0.78 \pm 0.03$. Although we could not evaluate the VOR compensation index in a similar fashion, the following discussion will attempt to provide a clearer understanding about the influence of the VOR gain on the compensation for the VOR-related portion of SED.

To understand the influence of the VOR gain $[g(f_H)]$ on CI, we computed the sensitivity of CI (the derivative of *Eq. 6*) to a variation in the VOR gain as follows

$$\frac{\partial \mathrm{CI}}{\partial g(f_H)} = (\mathrm{CI}^P - \mathrm{CI}^V) \times (1 - \mathrm{EC}) \qquad (12)$$

Equation 12 shows that (for EC <1), the sensitivity of CI to a variation in the VOR gain increases with EC. This can be explained more intuitively: the smaller the EC, the larger the contribution of the head to the SGD and therefore the larger the VOR component of SED. EC = 1 corresponds to a head-restrained condition and therefore *Eq. 12* shows that CI is insensitive to a change in the VOR gain. When EC >1, the relationship between a change in the VOR gain and CI is inverted compared with when EC <1. Unfortunately, as things are, this equation is insufficient because we do not know the VOR gain and can measure only the frequency of head movement. Therefore we evaluated the sensitivity of CI to head movement frequency as follows

$$\frac{\partial \mathrm{CI}}{\partial f_H} = \frac{\partial \mathrm{CI}}{\partial \hat{g}(f_H)} \frac{\partial \hat{g}(f_H)}{\partial f_H} \qquad (13)$$

Using *Eq. 12*, this results in an interpretable description of the head frequency-dependent compensation index

$$\frac{\partial CI}{\partial f_H} = (CI^P - CI^V) \times (1 - EC)\frac{\partial \hat{g}(f_H)}{\partial f_H} \quad (14)$$

Interestingly, *Eq. 14* now suggests that we should find a relationship between the overall compensation index and the head movement frequency. This is represented in Fig. 8*C* and shows that, indeed, the compensation index decreased with head movement frequency. Linear regression resulted in the following equation

$$CI = (-0.55 \pm 0.11) \times f_H + (0.96 \pm 0.12)$$

$$vaf = 0.44, P < 0.007 \quad (15)$$

In an analysis of subjects' individual performances, the slope of the regression varies in a range between 0.21 and −1.23. For all subjects, the slope was either not significantly different from zero ($n = 2$) or negative ($n = 6$). Comparing *Eq. 14* to *Eq. 15*, the correlation clearly could result only from the change of the VOR gain with head movement frequency. These sorts of changes were previously reported (Barnes 1993), such that with increasing head oscillation frequency, the VOR gain decreases.

The regression results from *Eq. 15* allowed us to further evaluate the sensitivity of the VOR gain to changes in head movement frequency. If we take *Eq. 14*, we now have only two unknown entities left: CI^V and $\partial\hat{g}(f_H)/\partial f_H$. We know CI^P from *Eq. 11* (see earlier text), EC can be evaluated from our data (i.e., the mean measured EC in our data set), and $\partial CI/\partial f_H$ (from *Eqs. 14* and *15*). Figure 9 represents the relationship between CI^V and the VOR gain sensitivity to head movement frequency. The confidence intervals take the variability of all parameters into account and thus present the worst-case scenario. Since CI^V values only between 0 and 1 make sense behaviorally, this graph allowed us to obtain an estimate of the VOR gain sensitivity to head movement frequency. For those values of CI^V, we found an upper limit on the value of $\partial\hat{g}(f_H)/\partial f_H$ that is equal to -0.365 ± 0.099 (mean ± 95% confidence interval). This means that the VOR gain changed linearly with a slope smaller than −0.365 in our range of head oscillation frequencies (0.6–1.2 Hz). An approximately linear relationship between the VOR gain and head movement frequency was previously reported for this range of frequencies (Barnes 1993), but the estimated slope was shallower, i.e., around −0.1. Using the data from Barnes, one can predict that CI^V should lie on the vertical dashed line represented in Fig. 9. Therefore our analysis suggests that the VOR gain was more sensitive to the head oscillation frequency during actively generated head movements as opposed to passive head rotations (Barnes 1993).

We conducted additional analyses to test whether the eye-in-head position, the head-in-space position, or the relative position of the flash with respect to the direction of the ongoing movement could significantly influence the compensation index. We found no statistically significant influence of those parameters on the compensation index.

DISCUSSION

In this study, we examined how visual constancy is maintained during head-unrestrained smooth pursuit. We found that during head-unrestrained pursuit, mechanisms are in play similar to those during head-restrained conditions. However, our data revealed a difference in the compensation gain for smooth eye displacements and head movements. Dividing the smooth eye displacements into smooth pursuit commands and VOR-related components, we estimated an interval for the rate of change of the VOR gain with respect to head movement frequency.

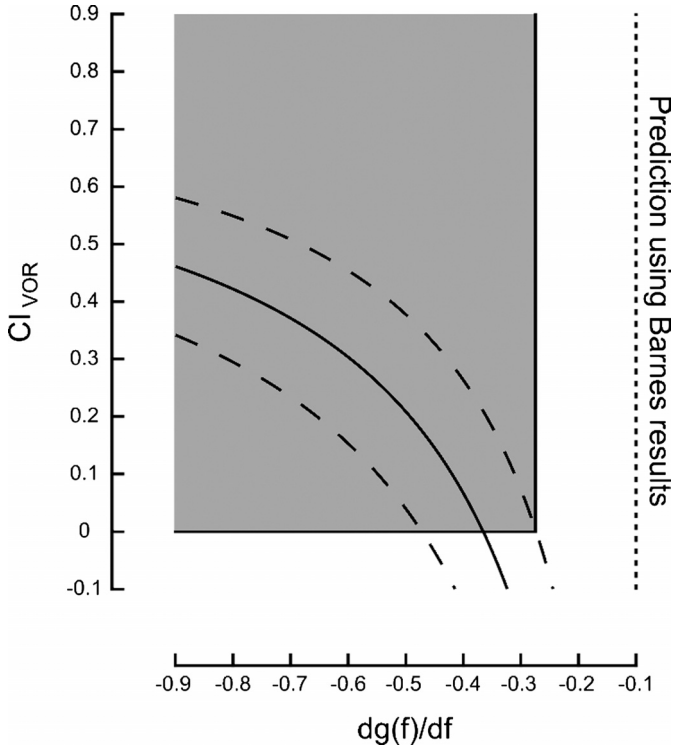

FIG. 9. VOR compensation index as a function of VOR gain sensitivity to a variation of head frequency. The X-axis represents the sensitivity of the gain of the VOR with respect to the head oscillation frequency. The Y-axis corresponds to the value of the compensation index for the VOR component of the eye command (see Fig. 2*B*). The gray box corresponds to the feasible domain for CI^V values. The right boundary of the gray box corresponds to the limit for which CI^V is >0 (sensitivity < −0.365). The dashed lines correspond to the 95% confidence intervals on the compensation index of the VOR component of the eye command. The vertical dashed line corresponds to the prediction that we can make if we use the data from Barnes (1993).

Compensation for smooth gaze displacements

We found that when subjects were asked to look at a briefly flashed target presented during head-unrestrained smooth pursuit, the brain was able to compensate for the smooth gaze movements that occurred during the saccadic latency period. Our analyses suggest that the general mechanisms of compensation for smooth eye displacements are similar to those observed in head-restrained conditions (Blohm et al. 2003, 2005a,b); thus short-latency gaze saccades were better correlated with retinal error at the flash presentation, whereas long-latency gaze saccades were better correlated with the spatial error at saccade onset (see Fig. 7, *A* and *B*). We found that the compensatory mechanism reached a plateau of roughly 62% of smooth gaze displacement compensation after about 400 ms. This result was in agreement with results previously reported during head-restrained pursuit (Blohm et al. 2005b). Those results indicated that the brain needs time to integrate

eye and head displacements during the latency period. This finding has also been interpreted in the past as evidence for a speed–accuracy trade-off (Blohm et al. 2005b).

Comparing the degree of compensation for smooth gaze displacements between head-restrained and head-unrestrained conditions, we observed very similar changes in the compensation index as a function of latency. However, a more detailed analysis revealed that, on average, the brain compensated for different percentages of smooth eye and head displacements, resulting in overall compensation values that largely depended on the contribution of the eye to the overall smooth gaze displacement. We showed that the eye contribution is independent with respect to the latency and that for each bin of eye contribution, the relationship between latency and compensation remains valid (Fig. 8, *B1–B3*; the longer the latency, the greater the compensation). It appears clearly that the latency is the predominant parameter that influences the compensation. We can only speculate as to why the compensation gain for head displacements during the latency period was smaller than the gain for smooth eye displacements. One possibility involves the fact that to maintain spatial constancy, the brain has to take into account both eye and head displacements (or compute their absolute position). Wang et al. (2007) showed that there is a proprioceptive representation of the eye-in-head position in area 3a of the somatosensory cortex. They concluded that there are two ways for the CNS to assess eye position: a rapid (but more sensitive to noise) corollary discharge and a slower (but more accurate) proprioceptive eye-in-head position in the somatosensory cortex. They proposed that the proprioceptive inputs may be used to "calibrate" the corollary discharge. As for head position, Blouin et al. (1995, 1998) used passive head rotation to show that the CNS has difficulty integrating vestibular signals to maintain spatial constancy. The authors of these studies argued that the CNS is not able to process the vestibular signals while fixating on a target in a head-fixed condition. It seems that, as is the case for eye position, there are two ways for the brain to have access to information about the head position: a fast one (which is noisier; Blouin et al. 1998) from the semicircular canals and a slow one using the proprioceptive neck inputs to compute head position. We propose that the brain has two choices linked to this speed–accuracy trade-off: either *1*) it can directly integrate the eye-velocity efference copy and the vestibular signal from the head to plan a gaze saccade or *2*) it can wait until an update of position comes from the proprioceptive inputs. This model could explain the observed speed–accuracy trade-off. It may seem strange that when the VOR gain is equal to one, any head movement is perfectly compensated by an eye movement whereas, conversely, the same head-velocity signal is not well integrated during spatial updating. However, we believe that the processing of vestibular information coming from the semicircular canals is totally different (in that it lasts longer and is more sensitive to noise) than that of the proprioceptive inputs in the computation of head position (displacement) driving eye movement during the VOR. This could explain why the CNS would rely more heavily on the less-noisy eye information than on head information to keep spatial constancy and why we observed a relationship between compensation and eye contribution. However, our data show that, with enough time to accurately compute the head displacement, the effect of EC on the compensation becomes less important. It is important to emphasize that authors have previously shown that vestibular signals are important in maintaining spatial constancy in monkeys (Wei et al. 2006). However, these authors used stationary targets, so the subject had no need of a speed–accuracy trade-off to decrease the influence of an intervening perturbing movement. Therefore it is difficult to distinguish the relative influence of the proprioceptive and vestibular inputs on the spatial constancy in this case.

Only a few studies have investigated spatial constancy in head-unrestrained conditions. It was previously shown (Medendorp and Crawford 2002; Medendorp et al. 2002b) that humans can (at least in part) update memorized targets across translational head movements between stationary targets. In another study (Medendorp et al. 2002a), subjects were presented with a flashed target after making a torsional rotation of the head while fixating on a central target. The subjects then had to null the head torsion and look at the memorized (and updated) flash position when the fixation target was extinguished. The mean elapsed duration between flash presentation and fixation extinction was around 2 s. The authors demonstrated that subjects perfectly compensated for the head torsion. It is difficult to compare the results from these studies to our results for a major reason: in Medendorp et al. (2002a), subjects had plenty of time to process signals coming from the semicircular canals and the proprioceptive inputs of the neck. There was no need for subjects to execute the movement quickly because there was no intervening movement acting as a perturbation during the planning of the gaze saccade.

In another study, Vliegen et al. (2005) studied head-unrestrained gaze saccade programming with a dynamic double-step paradigm. However, they addressed only how the saccadic system keeps track of its own movements, whereas we studied its interaction with the smooth pursuit system. Both their and our studies provide converging evidence that the brain uses dynamic retinal and extraretinal signals to keep track of self-motion.

In this study, we did not account for the 3D retinal geometry when performing our analysis of spatial constancy. Eye rotations can theoretically be executed around any rotational axis. Practically, the torsional component of the eye movement is defined by Listing's law (Tweed et al. 1990). Because of Listing's law, there is a rotational misalignment of retinal and spatial axes for oblique eye-in-head positions (Blohm and Crawford 2007; Crawford and Guitton 1997; Tweed et al. 1990). This rotation can yield a supplementary source of error if it is not taken into account by the updating mechanism during the programming of the gaze saccade. To test for a possible influence of the 3D retinal projection geometry on our results, we computed the amount of rotational misalignment for our data set, its mean ($\mu = -0.037°$) and its variance ($\sigma^2 = 0.39$ deg^2) using a previously described algorithm (Crawford and Guitton 1997). These values show that in our experiment the effects of 3D projection geometry were negligible compared with the magnitude of SGD. A more specific paradigm that allows the experimenter to obtain a larger range of angular misalignment would be necessary to precisely address the influence of the 3D retinal geometry on the spatial constancy mechanism. Because in our experiment subjects usually oriented their head with respect to the pursuit target using a roll rotation (data not shown), the updating mechanism of the flash position on the retina needs to take into account the

torsional part of the eye movement (ocular counter-roll) linked to the rotation of the head along the nasooccipital axis. It has been shown that passive (Klier et al. 2006) and active (Medendorp et al. 2002a) head roll rotations (and the accompanying ocular counter-roll) are taken into account during spatial updating of memorized targets. Based on these findings, we postulate that the torsional component of the eye movement shares the same properties for the integration as those of the horizontal and vertical components: the longer the latency, the greater the compensation.

In a study involving head-unrestrained tracking and gaze saccades, Herter and Guitton (1998) used a one-dimensional paradigm in which they first presented a flashed target while the subject was fixating on another target. Then subjects tracked a moving target with a combined eye–head movement. When the pursuit target extinguished, they had to look at the memorized (and updated) position of the flash. The authors of this study showed that subjects were able to accurately integrate smooth gaze displacements and update the memorized flash position to produce spatially accurate behavior.

VOR gain considerations

With a more detailed expression of the compensation index, we were able to make some predictions about the sensitivity of the VOR gain to the active head oscillation frequency. Our results suggest that the VOR gain is more sensitive to the head oscillation frequency during active head movement than during passive head rotations (Barnes 1993). Our predictions present supplementary evidence that there are major differences between an active and a passive head movement on the modulation of the VOR gain.

To stabilize gaze, the CNS needs to evaluate the head velocity and must dissociate an active head movement (during which the VOR must be negated and thus not be counterproductive) and a passive head movement (during which the VOR must be active to stabilize the gaze). The inputs used to evaluate head velocity in the present study are different from those in Barnes (1993). During the chair rotations used in the previous study (Barnes 1993), only the semicircular canals relay information about the head velocity. In contrast, during our head-unrestrained active movements, at least two sources are available to evaluate the head velocity: the output of the semicircular canals (proportional to the head-in-space velocity) and the proprioceptive discharge of the neck muscles (proportional to the head-on-trunk velocity). The difference in evaluation of the head velocity between the two cases may be an explanation of the important sensitivity of the gain of the VOR to the active head oscillation frequency.

In a series of experiments, Roy and Cullen (2004) showed the importance of dissociating active and passive components of head movement in understanding how the discharge of neurons in the vestibular nuclei is modulated. These authors proposed an expression that integrates the head-on-trunk and the head-in-space velocities to account for the discharge of vestibular neurons.

Making a parallel with the observations of Roy and Cullen (2004), we propose a mechanism to explain the differences between Barnes (1993) and our predictions. The sensitivity of the gain of the VOR to head oscillation frequency observed here may correspond to the active component of the firing rate modulation expression proposed by Roy and Cullen (2004). In contrast, Barnes (1993) observed the sensitivity of the gain to only the passive component of the expression.

Our result indicating that the gain of the VOR is less sensitive to passive head velocity than that to active head velocity seems to be reasonable. Generally, a passive head movement acts as a perturbation for the gaze and must be negated to keep the gaze stable. Thus it appears that the VOR gain must not be overly sensitive to variations in the passive head oscillation frequency. Conversely, an active head movement is usually not a perturbation during a gaze movement and therefore should not be negated systematically. During large head-unrestrained saccades Cullen et al. (2004), Lefèvre et al. (1992), and Tomlinson and Bahra (1986) all showed that the gain of VOR quickly decreases at the onset of a gaze saccade and rapidly increases before the end of the movement; therefore the VOR is not counterproductive during head-unrestrained saccade. The important sensitivity of the VOR gain during active head movements seems to be related to the modulation of the gain of VOR during head-unrestrained gaze shifts.

Additional experiments will be required to clarify how the VOR component is taken into account by the compensatory mechanism and to validate the proposed difference between active and passive head movements. Those experiments should include a more specific control of the gain of the VOR. This could be done by comparing, for example, the amount of compensation when subjects look at the same targets either on a rotating chair (passive head movement) or while making active head movements like those observed in this study.

Conclusion

In conclusion, we propose that there is a compensatory mechanism in head-unrestrained 2D tracking that takes into account the smooth gaze displacement occurring during the latency of a gaze saccade, similar to that of a head-restrained condition. In both conditions, the CNS needs some time to integrate the displacement. This integration time produces two different strategies: either the movement is realized as quickly as possible and relies on retinal error only at flash presentation (thus giving rise to an inaccurate gaze saccade) or the CNS takes the time to integrate the displacement realized during the latency and execute a more accurate gaze saccade. If the first saccade was inaccurate, we generally observed a second (or even a third) gaze saccade, which reduced the error. We also observed a relation between compensation and eye contribution: the greater the eye contribution, the greater the compensation. To explain this relationship, we proposed a simple model (see Fig. 2*B*) and showed that the gain of the VOR must change as a function of head oscillation frequency (see *Eq. 14*). From this link between head oscillation frequency and eye contribution, we deduced a relationship between head oscillation frequency and compensation of the smooth gaze displacement.

APPENDIX

Compensation indices: mathematical developments

In this section, we present the complete mathematical developments underlying the computation of the compensation indices presented herein.

We started with the first equation of the compensation. This equation states that the position error at the end of a saccade (PE) was a function of the smooth gaze displacement (SGD) that occurred during the latency and a compensation index (CI). CI corresponds to the amount of displacement that the compensatory mechanism has taken into account during the programming of the saccade

$$PE = SGD - CI \times SGD \quad (A1)$$

From *Eq.* A*1*, one can isolate CI

$$CI = \frac{SGD - PE}{SGD} \quad (A2)$$

The first stage was to decompose SGD into its head (SHD) and eye (SED) components

$$SGD = SHD + SED \quad (A3)$$

The same principle as that proposed in *Eq.* A*1* was used here for computation of the partial compensation for the eye displacement (CI^E) and the partial compensation for the head displacement (CI^H) during the saccade latency

$$PE = SGD - CI^E \times SED - CI^H \times SHD \quad (A4)$$

The purpose of the following developments was to obtain an expression that would allow a comparison of the partial compensation indices (CI^E and CI^H) with the global one (CI).

To begin, we defined the eye contribution (EC) as

$$EC = \frac{SED}{SGD} \quad (A5)$$

and the head contribution as

$$HC = \frac{SHD}{SGD} \quad (A6)$$

From *Eqs.* A*5* and A*6*, we can write

$$SED = EC \times SGD \quad (A7)$$

$$SHD = HC \times SGD \quad (A8)$$

$$HC = 1 - EC \quad (A9)$$

$$SHD = (1 - EC) \times SGD \quad (A10)$$

By inserting *Eqs.* A*7* and A*10* into *Eq.* A*4* we obtain

$$PE = SGD - CI^E \times EC \times SGD - CI^H \times (1 - EC) \times SGD \quad (A11)$$

As expected, from *Eq.* A*11*, the global CI can be expressed as a function of the partial compensation index for the eye (CI^E), the partial compensation index for the head (CI^H), and the eye contribution (EC)

$$\frac{SGD - PE}{SGD} = CI = CI^E \times EC + CI^H \times (1 - EC) \quad (A12a)$$

$$CI = (CI^E - CI^H) \times EC + CI^H \quad (A12b)$$

In a second stage for development of the compensation index, we divided SED into a pursuit and a VOR component

$$SED = SPD + VOR \quad (A13)$$

As in *Eq.* A*4*, this division allowed us to include two new compensation indices, one for the VOR signal (CI^V) and one for the pursuit component (CI^P)

$$PE = SGD - CI^P \times SPD - CI^V \times VOR - CI^H \times SHD \quad (A14)$$

Similar to the mathematical developments leading to *Eq.* A*12*, the purpose of the following series of expressions was to find an expression of the global compensation index as a function of the partial compensation indices. By inserting *Eq.* A*13* into *Eq.* A*14*, we obtained

$$PE = SGD - CI^P \times (SED - VOR) - CI^V \times VOR - CI^H \times SHD \quad (A15)$$

$$PE = SGD - CI^P \times SED + CI^P \times VOR - CI^V \times VOR - CI^H \times SHD \quad (A16)$$

$$PE = SGD - CI^P \times SED - (CI^V - CI^P) \times VOR - CI^H \times SHD \quad (A17)$$

As explained in the main text (METHODS, *Compensation*), the VOR signal was approximated by

$$VOR = -g(f_H) \times SHD \quad (A18)$$

Using *Eq.* A*18*, *Eq.* A*17* can be written as

$$PE = SGD - CI^P \times SED - (CI^P - CI^V) \times g(f_H) \times SHD - CI^H \times SHD \quad (A19)$$

By inserting *Eqs.* A*7* and A*10* into *Eq.* A*19*, we obtained

$$PE = SGD - CI^P \times EC \times SGD - (CI^P - CI^V) \times g(f_H) \times (1 - EC) \times SGD - CI^H \times (1 - EC) \times SGD \quad (A20)$$

$$PE = SGD - [CI^P - (CI^P - CI^V) \times g(f_H) - CI^H] \times EC \times SGD - [(CI^P - CI^V) \times g(f_H) + CI^H] \times SGD \quad (A21)$$

From *Eq.* A*20*, we isolate the global compensation index (CI) as a function of the three partial compensation indices (CI^V, CI^P, and CI^H), the gain of the VOR [$g(f_H)$], and the eye contribution (EC)

$$\frac{SGD - PE}{SGD} = CI = [CI^P - (CI^P - CI^V) \times g(f_H) - CI^H] \times EC + [(CI^P - CI^V) \times g(f_H) + CI^H] \quad (A22)$$

Equation A*22* corresponds to *Eq. 7* in the main text.

ACKNOWLEDGMENTS

We thank the subjects for participating in this study.

GRANTS

This work presents research results of the Belgian Network Dynamical Systems, Control, and Optimization, funded by the Interuniversity Attraction Poles Programme, initiated by the Belgian State, Science Policy Office. The scientific responsibility rests with its authors. P. Lefèvre was supported by the Fonds National de la Recherche Scientifique, Fondation pour la Recherche Scientifique Médicale, Actions de Recherche Concertées (French community, Belgium), Fonds Spéciaux de Recherche of the Université catholique de Louvain, European Space Agency (European Union [EU]), and Prodex Grant C90232 from Belgian Science Policy. G. Blohm was supported by a Marie

Curie Fellowship within the 6th Framework Program of the EU and NSERC (Canada).

REFERENCES

Angelaki DE, Cullen KE. Vestibular system: the many facets of a multimodal sense. *Annu Rev Neurosci* 31: 125–150, 2008.

Barnes GR. Visual-vestibular interaction in the control of head and eye movement: the role of visual feedback and predictive mechanisms. *Prog Neurobiol* 41: 435–472, 1993.

Basseville M, Nikiforov IV. *Detection of Abrupt Changes: Theory and Application*. Englewood Cliffs, NJ: Prentice Hall, 1993.

Berthoz A, Israel I, Georges-Francois P, Grasso R, Tsuzuku T. Spatial memory of body linear displacement: what is being stored? *Science* 269: 95–98, 1995.

Blohm G, Crawford JD. Computations for geometrically accurate visually guided reaching in 3-D space. *J Vis* 7: 1–22, 2007.

Blohm G, Missal M, Lefèvre P. Interaction between smooth anticipation and saccades during ocular orientation in darkness. *J Neurophysiol* 89: 1423–1433, 2003.

Blohm G, Missal M, Lefèvre P. Direct evidence for a position input to the smooth pursuit system. *J Neurophysiol* 94: 712–721, 2005a.

Blohm G, Missal M, Lefèvre P. Processing of retinal and extraretinal signals for memory-guided saccades during smooth pursuit. *J Neurophysiol* 93: 1510–1522, 2005b.

Blohm G, Optican LM, Lefèvre P. A model that integrates eye velocity commands to keep track of smooth eye displacements. *J Comput Neurosci* 21: 51–70, 2006.

Blouin J, Gauthier GM, van Donkelaar P, Vercher JL. Encoding the position of a flashed visual target after passive body rotations. *Neuroreport* 6: 1165–1168, 1995.

Blouin J, Labrousse L, Simoneau M, Vercher JL, Gauthier GM. Updating visual space during passive and voluntary head-in-space movements. *Exp Brain Res* 122: 93–100, 1998.

Carpenter RH, Williams ML. Neural computation of log likelihood in control of saccadic eye movements. *Nature* 377: 59–62, 1995.

Crawford JD, Guitton D. Visual-motor transformations required for accurate and kinematically correct saccades. *J Neurophysiol* 78: 1447–1467, 1997.

Cullen KE, Huterer M, Braidwood DA, Sylvestre PA. Time course of vestibuloocular reflex suppression during gaze shifts. *J Neurophysiol* 92: 3408–3422, 2004.

de Brouwer S, Missal M, Barnes G, Lefèvre P. Quantitative analysis of catch-up saccades during sustained pursuit. *J Neurophysiol* 87: 1772–1780, 2002a.

de Brouwer S, Missal M, Lefèvre P. Role of retinal slip in the prediction of target motion during smooth and saccadic pursuit. *J Neurophysiol* 86: 550–558, 2001.

de Brouwer S, Yuksel D, Blohm G, Missal M, Lefèvre P. What triggers catch-up saccades during visual tracking? *J Neurophysiol* 87: 1646–1650, 2002b.

Diks C, Manzan S. Tests for serial independence and linearity based on correlation integrals. *Stud Nonlinear Dynam Economet* 6: Article 2, 2002.

Hallett PE, Lightstone AD. Saccadic eye movements to flashed targets. *Vision Res* 16: 107–114, 1976a.

Hallett PE, Lightstone AD. Saccadic eye movements towards stimuli triggered by prior saccades. *Vision Res* 16: 99–106, 1976b.

Herter TM, Guitton D. Human head-free gaze saccades to targets flashed before gaze-pursuit are spatially accurate. *J Neurophysiol* 80: 2785–2789, 1998.

Israel I, Grasso R, Georges-François P, Tsuzuku T, Berthoz A. Spatial memory and path integration studied by self-driven passive linear displacement. I. Basic properties. *J Neurophysiol* 77: 3180–3192, 1997.

Klier EM, Angelaki DE. Spatial updating and the maintenance of visual constancy. *Neuroscience* 156: 801–818, 2008.

Klier EM, Angelaki DE, Hess BJ. Roles of gravitational cues and efference copy signals in the rotational updating of memory saccades. *J Neurophysiol* 94: 468–478, 2005.

Klier EM, Hess BJ, Angelaki DE. Differences in the accuracy of human visuospatial memory after yaw and roll rotations. *J Neurophysiol* 95: 2692–2697, 2006.

Krauzlis RJ, Miles FA. Decreases in the latency of smooth pursuit and saccadic eye movements produced by the "gap paradigm" in the monkey. *Vision Res* 36: 1973–1985, 1996.

Lanman J, Bizzi E, Allum J. The coordination of eye and head movement during smooth pursuit. *Brain Res* 153: 39–53, 1978.

Lefèvre P, Bottemanne I, Roucoux A. Experimental study and modeling of vestibulo-ocular reflex modulation during large shifts of gaze in humans. *Exp Brain Res* 91: 496–508, 1992.

McKenzie A, Lisberger SG. Properties of signals that determine the amplitude and direction of saccadic eye movements in monkeys. *J Neurophysiol* 56: 196–207, 1986.

Medendorp WP, Crawford JD. Visuospatial updating of reaching targets in near and far space. *Neuroreport* 13: 633–636, 2002.

Medendorp WP, Smith MA, Tweed DB, Crawford JD. Rotational remapping in human spatial memory during eye and head motion. *J Neurosci* 22: RC196, 2002a.

Medendorp WP, Van Gisbergen JA, Gielen CC. Human gaze stabilization during active head translations. *J Neurophysiol* 87: 295–304, 2002b.

Ronsse R, White O, Lefèvre P. Computation of gaze orientation under unrestrained head movements. *J Neurosci Methods* 159: 158–169, 2007.

Roy JE, Cullen KE. Vestibuloocular reflex signal modulation during voluntary and passive head movements. *J Neurophysiol* 87: 2337–2357, 2002.

Roy JE, Cullen KE. Dissociating self-generated from passively applied head motion: neural mechanisms in the vestibular nuclei. *J Neurosci* 24: 2102–2111, 2004.

Sauter D, Martin BJ, Di Renzo N, Vomscheid C. Analysis of eye tracking movements using innovations generated by a Kalman filter. *Med Biol Eng Comput* 29: 63–69, 1991.

Schlag J, Schlag-Rey M. Through the eye, slowly: delays and localization errors in the visual system. *Nat Rev Neurosci* 3: 191–200, 2002.

Schlag J, Schlag-Rey M, Dassonville P. Saccades can be aimed at the spatial location of targets flashed during pursuit. *J Neurophysiol* 64: 575–581, 1990.

Tomlinson RD, Bahra PS. Combined eye–head gaze shifts in the primate. II. Interactions between saccades and the vestibuloocular reflex. *J Neurophysiol* 56: 1558–1570, 1986.

Tweed D, Cadera W, Vilis T. Computing three-dimensional eye position quaternions and eye velocity from search coil signals. *Vision Res* 30: 97–110, 1990.

Vliegen J, Van Grootel TJ, Van Opstal AJ. Gaze orienting in dynamic visual double steps. *J Neurophysiol* 94: 4300–4313, 2005.

Wang X, Zhang M, Cohen IS, Goldberg ME. The proprioceptive representation of eye position in monkey primary somatosensory cortex. *Nat Neurosci* 10: 640–646, 2007.

Wei M, Li N, Newlands SD, Dickman JD, Angelaki DE. Deficits and recovery in visuospatial memory during head motion after bilateral labyrinthine lesion. *J Neurophysiol* 96: 1676–1682, 2006.